J|A|C|S
ARTICLES
Published on Web 01/31/2006

A Europium Complex That Selectively Stains Nucleoli of Cells

Junhua Yu,[†] David Parker,*[,†] Robert Pal,[†] Robert A. Poole,[†] and Martin J. Cann[‡]

Contribution from the Department of Chemistry and School of Biological and Biomedical Sciences, Durham University, South Road, Durham DH1 3LE, United Kingdom

Received September 13, 2005; E-mail: david.parker@durham.ac.uk

Abstract: A europium complex selectively staining the nucleolus of NIH 3T3, HeLa, and HDF cells is reported. This complex possesses not only the advantage of the long lifetime of europium emission (0.3 ms), but also a chromophore that allows excitation at a relatively long wavelength ($\lambda_{max} = 384$ nm) and gives rise to an acceptable quantum yield (9%). The complex can be used both in live cell and fixed cell imaging, giving an average intracellular concentration on the order of 0.5 μM. Strong binding to serum albumin has been demonstrated by examination of the analogous gadolinium complex, studying relaxivity changes with increasing protein concentration. The intracellular speciation of the complex has been examined by circularly polarized emission spectroscopy and is consistent with the presence of more than one europium species, possibly protein bound.

Introduction

The nucleolus of the cell was discovered over a century ago, yet its biological roles remain to be fully elucidated.[1] It is widely accepted that nucleoli are nuclear sites of ribosomal RNA transcription, processing, and ribosome assembly.[2] The nucleolus is a dynamic nuclear compartment formed during interphase through fusion of initially separate nucleolar materials. The mechanisms inducing the conglutination of various nucleolar components are still under investigation.[3] Alternative functions to a role in ribosome biogenesis have been proposed; for example, signal recognition, particle RNA maturation, a potential role for growth factors and growth-factor-related proteins, and potential links between nucleoli and tumorigenesis and aging have also been postulated.[4] The nucleolus may also be the target of certain viruses.[5]

Studies of nucleoli and nucleolus-related processes often require the visualization of nucleoli. Silver nitrate staining of a group of argyrophilic proteins highlights the nucleolar organizer regions (NORs) and partially exposes the localization of the nucleolus.[6] However, the limited staining exhibited as dark spots under light microscopy has inhibited widespread application, especially multicolor fluorescent labeling experiments. The most extensively used methods to stain the nucleolus require the employment of antibodies against a certain component of the nucleolus. For example, the anti-fibrillarin monoclonal antibody has been loaded into cells to indicate the localization of nucleoli.[7] An advantage of this method is the specificity of the antibody against its antigen, allowing researchers to examine the salient targeted biomolecules or processes. However, this requires not only a specific antibody that is usually expensive and often not commercially supplied, but also another dye that needs to be conjugated to this antibody, or even an "anti-antibody" antibody to detect this antibody.[8] Though there are reports employing green fluorescent protein (GFP),[9] the development of stable mammalian cell lines expressing GFP fusion proteins remains demanding work.[10] Low MW molecular probes for nucleoli are very rare. The only commercial nucleolar stain is "SYTO RNA-Select", a green fluorescent cell stain.[11] This dye gives rise to an enhanced fluorescence on binding to RNA.

Compared to common organic fluorescent dyes and semiconductor quantum dots (QDs), lanthanide complexes have the advantage of a long luminescence lifetime, large Stokes shift, and relatively high quantum yield. The latter feature is achieved when appropriate sensitizers are incorporated into the structure,

[†] Department of Chemistry.
[‡] School of Biological and Biomedical Sciences.

(1) Leung, A. K. L.; Andersen, J. S.; Mann, M.; Lamond, A. I. *Biochem. J.* **2003**, *376*, 553.
(2) Yusupov, M. M.; Yusupova, G. Zh.; Baucom, A.; Lieberman, K.; Earnest, T. N.; Cate, J. H. D.; Noller, H. F. *Science* **2001**, *292*, 883.
(3) Scheer, U.; Hock, R. *Curr. Opin. Cell Biol.* **1999**, *11*, 365.
(4) (a) Jacobson, M. R.; Pederson. T. *Proc. Natl. Acad. Sci. U.S.A.* **1998**, *95*, 7981. (b) Pederson, T. *J. Cell Biol.* **1998**, *143*, 279. (c) Grummt, I. *Genes Dev.* **2003**, *17*, 1691. (d) Johnson, F. B.; Marciniakt, R. A.; Guarente, L. *Curr. Opin. Cell Biol.* **1998**, *10*, 332.
(5) Hiscox, J. A. *Arch. Virol.* **2002**, *147*, 1077.
(6) Derenzini M. *Micron* **2000**, *31*, 117.
(7) (a) Dean, K. A.; von Ahsen, O.; Görlich, D.; Fried, H. M. *J. Cell Sci.* **2001**, *114*, 3479. (b) Korgaonkar, C.; Hagen, J.; Tompkins, V.; Frazier, A. A.; Allamargot, C.; Quelle, F. W.; Quelle, D. E. *Mol. Cell. Biol.* **2005**, *25*, 1258.
(8) (a) Lin, C.-Y.; Li, C.-C.; Huang, P.-H.; Lee, F.-J. S. *J. Cell Sci.* **2002**, *115*, 4433. (b) Leary, D. J.; Terns, M. P.; Huang, S. *Mol. Cell. Biol.* **2004**, *15*, 281. (c) Leopardi, R.; Roizman, B. *Proc. Natl. Acad. Sci. U.S.A.* **1996**, *93*, 4572.
(9) Snaar, S.; Wiesmeijer, K.; Jochemsen, A. G.; Tanke, H. J.; Dirks, R. W. *J. Cell Biol.* **2000**, *151*, 653.
(10) Spector, D. L.; Goldman, R. D. In *Live Cell Imaging: A Laboratory Manual*; Goldman, R. D., Spector, D. L., Eds.; Cold Spring Harbor: New York, 2005; pp 25−31.
(11) (a) Haugland, R. P. *A Guide to Fluorescent Probes and Labeling Technologies*, 10th ed.; Molecular Probes: Eugene, OR, 2005. Parker, D. *Coord. Chem. Rev.* **2000**, *205*, 109; Pandya, S.; Yu, J.; Parker, D. *Dalton Trans.*, in press. (b) Phimphivong, S.; Saavedra, S. S. *Bioconjugate Chem.* **1998**, *9*, 350. (c) Gao, X.; Yang, L.; Petros, J. A.; Marshall, F. F.; Simons, J. W.; Nie, S. *Curr. Opin. Biotechnol.* **2005**, *16*, 63. Bruchez, M., Jr.; Moronne, M.; Gin, P.; Weiss, S.; Alivisatos, A. P. *Science* **1998**, *281*, 2013. Jaiswal, J. K.; Simon, S. M. *Trends Cell Biol.* **2004**, *14*, 497. (d) Cha, A.; Snyder, G. E.; Selvin, P. R.; Bezanilla, F. *Nature* **1999**, *402*, 809. Root, D. D. *Proc. Natl. Acad. Sci. U.S.A.* **1997**, *94*, 5685. Maurel, D.; Kriazeff, J.; Mathis, G.; Trinquet, E.; Ansanay, H. *Anal. Biochem.* **2004**, *329*, 253.

10.1021/ja056303g CCC: $33.50

Scheme 1. Synthesis of the Europium Complex $[EuL]^{3+}$

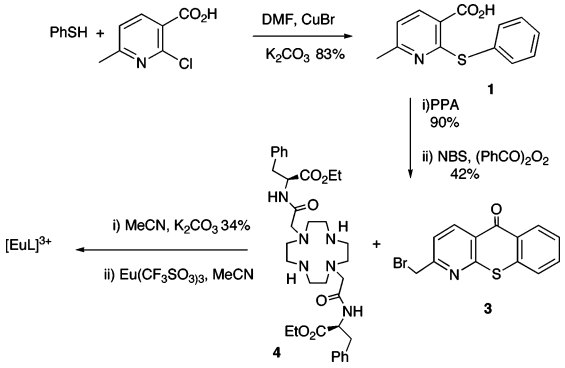

allowing intramolecular energy transfer to, for example, the europium(III) ion.[11a] The development of time-gated microscopy renders lanthanide complexes even more attractive as probes, by virtue of their micro- to millisecond lifetime.[11b] The large Stokes shift (excitation in the near UV and emission in the green or red) and narrow half-height peak widths (<10 nm) are particularly useful for multicolor imaging. Moreover, while QDs are considered more stable to photobleaching, their large volumes and poor cell permeability may limit their utility.[11c] Luminescent lanthanide complexes have been applied as fluorescence resonance energy transfer (FRET) donors in the study of a variety of extracellular processes.[11d] However, the investigation of their cell imaging properties is virtually unexplored.

Here, we report the surprising behavior of a europium(III) complex ($[EuL]^{3+}$) which may constitute a good alternative to the commercial nucleolar stain. Not only does it possess a red

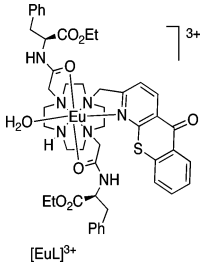

emission contrasting with the green fluorescence of SYTO RNA-Select (for multicolor imaging), but the complex also possesses a long emission lifetime, avoiding autofluorescence from biomolecules when using time-gating microscopy. The complex was originally studied for its ability to act as a chemosensor for anions, binding the citrate anion with very good chemoselectivity in competitive media.[12]

Results and Discussion

Synthesis. The synthesis of the macrocyclic ligand, L, followed standard methods. Reaction of thiophenol with 2-chloro-6-methylnicotinic acid gave the thioether **1** (Scheme 1), which underwent electrophilic cyclization in the presence of poly(phosphoric acid) to yield the azathioxanthone. Selective bromination of the benzylic site (NBS/AIBN/CCl_4) gave the mono(bromomethyl) derivative **2**. Controlled alkylation of the *trans*-disubstituted cyclen diamide **3** (K_2CO_3, MeCN) afforded

(12) (a) Parker, D.; Yu, J. *Chem. Commun.* **2005**, 3141. The binding affinity of [EuL] for citrate reported is 3×10^6 M^{-1}, and in a simulated extracellular ionic background, K_d is 0.28 mM. (b) Osaki, F.; Kanamori, T.; Sando, S.; Sera, T.; Aoyama, Y. *J. Am. Chem. Soc.* **2004**, *126*, 6520.

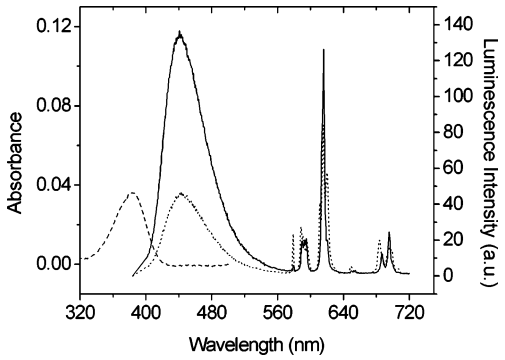

Figure 1. Absorption (dashed line) and total emission spectra of $[EuL]^{3+}$ (5 μM) in water (dotted line) and in the presence of L-Asn (solid line, pH 7.3, 300 μM).

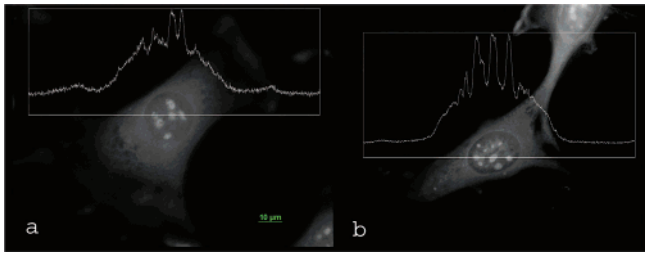

Figure 2. Luminescence images of NIH 3T3 cells loaded with $[EuL]^{3+}$: (a) cells incubated with the complex (500 μM, 1 h) in DMEM, (b) the same as (a) but the cells were prefixed by methanol. Images were taken on a Zeiss Axiovert 200M epifluorescence microscope, examining thioxanthone fluorescence with a GFP filter setting (objective, Plan-Apochromat, 63×/1.40 oil DIC; excitation filter, band-pass 450 ± 30 nm; emission filter, band-pass 510 ± 25 nm). Scale bar: 10 μm.

the desired ligand, L, in modest yield after purification by alumina chromatography. The Eu(III) complex was isolated following reaction with anhydrous europium(III) trifluoromethanesulfonate in MeCN.

As reported in our previous work,[12] sensitized emission of the aqua complex of $[EuL]^{3+}$ (Figure 1) has a quantum yield of 9% in water, about one-fifth of the fluorescence quantum yield for the thioxanthone chromophore, following excitation at 384 nm. The luminescence lifetime of the europium ion is 0.30 ms, much longer than the usual fluorescence lifetimes of organic dyes (nanosecond scale).

Cell Localization Behavior. The complex $[EuL]^{3+}$ permeates into NIH 3T3, HeLa, and HDF cells when the complex is loaded in DMEM (Dulbecco's modified Eagle's medium) with 10% NBS (natal bovine serum) at 37 °C in 5% CO_2/air. Some bright spots are then evident in the nuclei of cells excited by near-UV light (epifluorescence microscopy; excitation filter, band-pass 450 ± 30 nm; emission filter, 510 ± 25 nm). Moreover, pale luminescence can also be observed in the nucleus and cytoplasm (Figure 2a). Loading concentrations down to 100 μM were examined and found to achieve bright luminescence images of cells (see the Supporting Information, Figures 1S and 2S). The use of time-gating microscopy or epifluorescence microscopy equipped with better filters for europium ion emission (excitation filter, 380 ± 10 nm; emission filter, LP 550 nm) will lower the concentration required and increase the signal/noise ratio.

A key consideration is whether the cells studied remain viable and healthy over the period of examination. From the bright field images, more than 90% of the cells were considered to be healthy, over a 24 h period, when the loading concentration of $[EuL]^{3+}$ was 100 μM. The observation of the nucleolus over

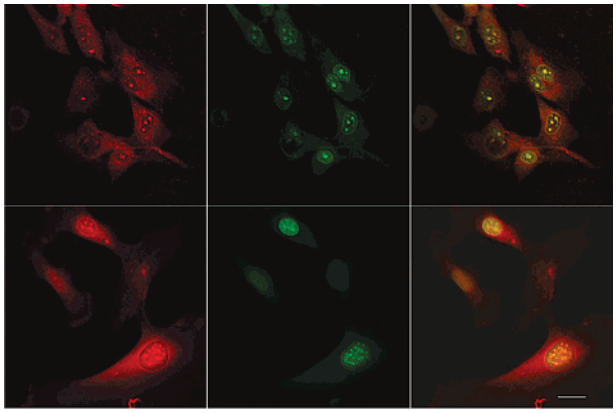

Figure 3. Colocalization of $[EuL]^{3+}$ and SYTO RNA-Select dye: upper row, images by live cell loading (complex (100 μM, 4 h) and SYTO dye (500 nM, 30 min)); lower row, images by fixed cell loading (similar to the upper row but the cells were fixed before complex loading); left column, Eu^{3+} luminescence; middle column, SYTO dye fluorescence; right column, merged image. Images were taken using a Zeiss LSM 500 META confocal microscope (for europium luminescence, excited at 405 nm, detected after filtration with an LP 505 filter; for the SYTO dye, excited at 488 nm, Ar laser, detected after filtration with a BP 505-550 band-pass filter). Scale bar: 20 μm.

such extended time periods provides strong evidence that the observed cells are healthy. Cell viability experiments were undertaken, coloading with calcein-AM, a dye used to assess cell viability in most eukaryotic cells. In live cells, the nonfluorescent calcein-AM is converted to green fluorescent calcein, following acetoxymethyl ester hydrolysis catalyzed by intracellular esterases. Cells were examined by microscopy using appropriate excitation and emission filters so that the red europium and green calcein emission could be examined separately. Cells loaded with complex or calcein-AM only were used as a control. For the coloaded cells (500 μM complex, 3 h of loading), green and red emission was observed in >97% of the cells examined, consistent with good cell viability.

When the complex was loaded at 4 °C, europium luminescence was still clearly observed, indicating that the complex is unlikely to enter the cells by endocytosis. The relatively even distribution of the complex in the cytoplasm also supports this premise. Molecules and conjugates entering cells via endocytosis are believed to be initially trapped in endocytotic vesicles and then transferred into endosomes. Only molecules and conjugates escaping from the endocytosis pathway can survive to act as probes.[12b]

Colocalization experiments were undertaken to confirm that the bright spots observed in the nucleus were related to the luminescence of the complex localizing at the nucleolus (Figure 3). Live cells were loaded with the complex or the commercially available nucleolar stain SYTO RNA-Select. The bright spots of the image (upper row, red), i.e., the luminescence of the europium complex (excited here by a laser at 405 nm and detected after filtration with an LP 505 nm filter; N.B. only the emission of the europium ion can be recorded at this setting), colocalize with those (upper row, green) obtained at the setting for SYTO RNA-Select dye (excited at 488 nm, Ar laser, detected after filtration with a BP 505-550 filter). The colocalization is evident as the bright yellow spots at the nucleoli, after merging (upper row, right column, Figure 3). This strongly suggests that the targeted organelles are the nucleoli and that the observed luminescence derives from the europium complex.

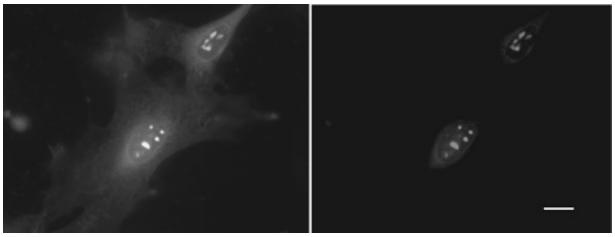

Figure 4. The NIH 3T3 cells were incubated in the presence of the complex (500 μM) in DMEM for 4 h. Images were taken here showing thioxanthone fluorescence on a Zeiss Axiovert 200M epifluorescence microscope (objective, Plan-Apochromat, 63×/1.40 oil DIC; excitation filter, BP 450 ± 30 nm; emission filter, BP 510 ± 25 nm). Acquisition time: left panel, 230 ms; right panel, 100 ms. Scale bar: 14 μm.

Parallel observations were made with HeLa cells (human endothelial carcinoma cells; see the Supporting Information, Figure 11S) and HDF cells (human dermal fibroblasts, a nontransformed primary cell line with a lower nucleolar number, Supporting Information, Figure 12S), with localization also clearly evident in the nucleoli. The consistent and stable luminescence of the complex in live cells renders the complex a new candidate for live cell imaging.

Though live cell imaging is rapidly developing,[13] fixed cells are still frequently used.[14] The complex can also be applied to visualize fixed cells as shown in Figure 2b. The cells were fixed using methanol, resulting in luminescence characteristics similar to those found in live cell loading. In the profiles shown in Figure 2, the light intensity of the nucleoli, from both fixed cell loading and live cell loading, is 3 times higher than that in the cytoplasm and 2 times higher than that of the nuclear membrane. This intensity profile permits the attainment of an exclusive image of the nucleolus by adjusting the excitation intensity or the gain value of the microscope (Figure 4).

The cells were fixed in methanol, resulting in luminescence characteristics similar to those found in live cell loading. In the profiles shown in Figure 2, the light intensity of the nucleoli, from both fixed cell loading and live cell loading, is 3 times higher than that in the cytoplasm and 2 times higher than that of the nuclear membrane. This intensity profile permits the attainment of an exclusive image of the nucleolus by adjusting the excitation intensity or the gain value of the microscope (Figure 4).

The number of the nucleoli in the cell depends on its mitotic stage and its health status. The nucleolus is visible before mitosis (interphase), dissolves at prophase, and then becomes discernible again at telophase.[15] As is evident from the images, almost all cells examined have more than two nucleoli. This is consistent with the fact that NIH 3T3 cells,[16] like some malignant cells, may have a higher nucleolus number, related to cell proliferative activity.[17] For the nontransformed HDF cells, on the other hand, a single nucleolus was typically observed.

The colocalization of fixed cells loaded with the complex and the SYTO dye demonstrates the excellent potential for this

(13) (a) Shav-Tal, Y.; Singer, R. H.; Darzacq, X. *Nat. Rev. Mol. Cell Biol.* **2004**, *5*, 855. (b) Watson, P.; Jones, A. T.; Stephens, D. J. *Adv. Drug Delivery Rev.* **2005**, *57*, 43.
(14) *Molecular Biology of the Cell*, 4th ed.; Alberts, B., Johnson, A., Lewis, J., Raff, M., Roberts, K., Walter, P., Eds.; Garland Science: New York, 2002; Chapter 9.
(15) Stevens, B. J. *J. Cell Biol.* **1965**, *24*, 349.
(16) Jainchill, J. L.; Aaronson, S. A.; Todaro, G. J. *J. Virol.* **1969**, *4*, 549.
(17) Horky, M.; Kotala, V.; Anton, M.; Wesierska-Gadek, J. *Ann. N. Y. Acad. Sci.* **2002**, *973*, 258.

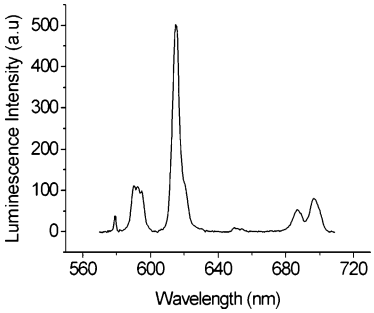

Figure 5. Luminescence spectrum of NIH 3T3 cells loaded with the complex. The cells at 80% confluency were loaded with the complex (200 μM) for 5 h, washed with PBS eight times, and then harvested with trypsin. The mixture was centrifuged, and the pellet was resuspended in PBS (1.5 mL) for spectral measurement. The cells loaded with the complex were excited at 384 nm. The final spectrum was "baseline corrected".

complex as a nucleolus stain. The fluorescence image of fixed cells loaded with the SYTO dye is slightly different from that obtained by live cell loading. The latter shows more intense localization of the dye in the whole nucleus compared to its cytoplasm distribution, and the bright spots (nucleoli) are not quite so clearly distinguished. Overall, the complex behaves similarly in each method (Figure 3).

Complex Concentration and Speciation. The average concentration of the complex in cells was estimated by measuring the concentration of europium in a given cell cohort. By harvesting cells loaded with the complex (200 μM for 5 h) in a 100 mm Petri dish following treatment with trypsin, the number of labeled cells suspended in a 0.4 mL volume of PBS (phosphate-buffered saline) was counted using laser sorting flow cytometry. The total concentration of europium in this sorted sample (71400 cells) was measured by ICP optical emission spectroscopy. Given that the studied NIH 3T3 cell may be estimated to have a mean volume of 4000 μm^3, each cell was calculated to contain 2×10^{-15} mol of Eu (1.2×10^9 Eu complexes), equivalent to an intracellular concentration of 0.5 μM.

As reported earlier, the emission of the complex is particularly sensitive to citrate, with the ratio of the luminescence intensity of the $\Delta J = 2$ (616 nm) to $\Delta J = 0$ (579 nm) bands increasing from 3.5 to reach a limiting value of 22.[12] In addition, L-Asp, L-Asn, and malate, each with a 2-hydroxy/amino-1,4-butanedicarboxylate structure, have a similar influence on the emission spectrum of $[EuL]^{3+}$ (Figure 1 and unpublished data). At the same time, other common biological anions, such as lactate, phosphate, bicarbonate, ATP, ADP, AMP, and chloride, change this ratio only slightly, the value remaining around 3.5. The addition of t-RNA, CT-DNA, and serum albumin to the aqueous solution of the complex decreased the luminescence intensity of the complex (see the Supporting Information, Figures 3S−8S). On the other hand, the presence of citrate in the mixture of DNA/RNA or protein and the complex gave rise to the characteristic emission of the citrate adduct, no matter which species (nucleic acid/protein or citrate) was added first.

The luminescence spectrum of the complex localized in cells exhibits a ratio of the bands centered at 618 and 580 nm ($\Delta J = 2/\Delta J = 0$ ratio) of 15 ± 1 (Figure 5), consistent with a ternary adduct involving binding to a species that is structurally similar to citrate. This ternary "complex" may also undergo reversible binding to an endogenous protein. To address this aspect further,

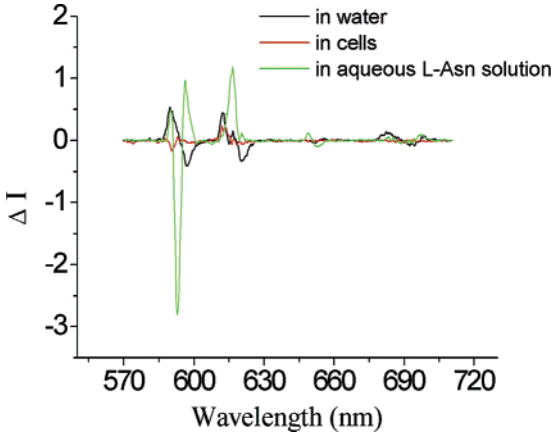

Figure 6. CPL spectrum of $[EuL]^{3+}$ in aqueous solution (black), in cells (red), and in aqueous L-Asn solution (green). The concentrations of the complex and L-Asn are 5 and 300 μM, respectively; the cells were the same sample as described in Figure 5. The excitation wavelength was 384 nm.

the corresponding Gd complex was prepared and its relaxivity determined in the absence and presence of serum albumin, a protein present both in the cell growth medium and within the cell. The relaxivity of $[GdL]^{3+}$ was measured to be 7.1 mM^{-1} s^{-1} (37 °C, 60 MHz) as the triflate salt and 5.2 mM^{-1} s^{-1} as the citrate adduct. Incremental addition of protein to a 0.1 mM solution containing the complex caused the relaxivity to rise steeply. In the presence of 0.1 mM serum albumin the relaxivity increased to 54 mM^{-1} s^{-1}. Further addition of protein caused no significant relaxivity change. When citrate (0.1 mM final concentration) was added to this solution, the relaxivity fell to 16.2 mM^{-1} s^{-1}, and the inverse addition experiment gave a solution with a relaxivity of 13 mM^{-1} s^{-1}. Taken together, these behaviors are consistent with reversible binding of the complex to the protein as suggested in the luminescence experiments. Citrate binds preferentially to the Eu complex in the presence of protein. The citrate adduct itself ($q = 0$) also binds to protein, giving rise to a smaller relaxivity enhancement in the ternary adduct.

Circularly polarized luminescence (CPL) spectroscopy can also be a good fingerprint of europium complex speciation.[18] CPL spectra for **[**$EuL]^{3+}$ were recorded in the presence of citrate, L-Asp, L-Asn, malate, and oxalate and for the complex localized in the NIH 3T3 cells (Figure 6). The latter spectrum did not match well with any single-component adduct (see also Figures 9S and 10S in the Supporting Information), the observed spectrum partially exhibiting characteristics of the adduct with L-Asn (negative band at 592 nm, positive band in the $\Delta J = 2$ manifold). Taken together, the spectral studies are consistent with intracellular formation of one or more europium complexes in which the bound waters have been displaced, forming one or more ternary species with a doubly or triply charged anion (probably not simply citrate itself, nor any simple phosphoanion), each of which is likely to be structurally related to α-hydroxy/α-amino-1,4-dicarboxylic acid derivatives.

Conclusions

A cationic europium(III) complex has been defined with surprisingly good and selective staining of the nucleolus of NIH

(18) (a) Bruce, J. I.; Dickins, R. S.; Govenlock, L. J.; Gunnlaugsson, T.; Lopinski, S.; Lowe, M. P.; Parker, D.; Peacock, R. D.; Perry, J. J. B.; Aime, S.; Botta M. *J. Am. Chem. Soc.* **2000**, *122*, 9674. (b) Atkinson, P.; Bretonniere Y.; Parker, D.; Muller, G. *Helv. Chim. Acta* **2005**, *88*, 391.

3T3, HeLa, and HDF cells. This complex can be used in both live cell imaging and fixed cell imaging, with the advantages of the red emission and the long luminescence lifetime of the europium ion. This behavior serves to highlight the opportunities available for the definition of new families of emissive lanthanide complexes, suitable for use in selective cell staining experiments and amenable to examination by time-resolved microscopy.

Experimental Section

General Remarks. All the solvents were distilled before use. All the other reagents (Aldrich-Sigma) were used as received. RNA-Select green fluorescent cell stain was obtained from Molecular Probes. UV/vis spectra and luminescence spectra were recorded with a Perkin-Elmer spectrometer (UV/vis/NIR Lambda 900) and Fluorolog-3 spectrometer (Horiba- Jobin Yvon) in a 1 cm optical path quartz cell at room temperature, respectively. Silica gel (TLC standard grade, Aldrich) was used for column chromatography. ESI-MS spectra were recorded using a VG Platform II electrospray mass spectrometer. Accurate masses were determined on a Thermo-Finnigan LTQ FT mass spectrometer. ^{1}H and ^{13}C NMR was recorded on a Bruker Avance-400 (400 MHz), Varian Mercury-200 (200 MHz), or Varian Unity-500 (500 MHz) instrument. Epifluorescence images were taken on a Zeiss Axiovert 200M epifluorescence microscope with a digital camera; confocal images were taken on a Zeiss LSM 500 META confocal microscope with 405 nm diode laser excitation and an LP 505 emission filter for europium complex luminescence and with 488 nm argon laser excitation and a BP 505-550 filter for SYTO dye fluorescence. Flow cytometric analysis and sorting was conducted using a DakoCytomation Inc. MoFlo multilaser flow cytometer (Fort Collins, CO). Samples were interrogated with a 100 mW 488 nm solid-state laser (FSC, SSC) and a 104 mW 351/363 nm argon ion laser. Fluorescence signals were detected through an interference filter centered at 450 nm with a 65 nm band-pass. Fluorescence signals were collected in the logarithmic mode. The data were analyzed using Summit v4.0 (DakoCytomation) software. CPL spectra were measured at the University of Glasgow, as reported previously,[18] with the assistance of Dr. R. D. Peacock. Inductively coupled plasma optical emission spectroscopic measurements to determine Eu concentration were made using a Jobin-Yvon Ultima 2 spectrometer. Relaxivity measurements were made at 37 °C and 60 MHz on a Bruker Minispec mq60 instrument. The mean value of three separate measurements was recorded.

Ligand and Complex Synthesis. 6-Methyl-2-thiophenoxynicotinic acid, 1. 2-Chloro-6-methylnicotinic acid (5.00 g, 29.2 mmol) and thiophenol (3.80 g, 34.5 mmol) were dissolved in DMF (30 cm^3) with stirring, followed by copper(I) bromide (0.25 g, 17.5 mmol) and K_2CO_3 (6.00 g, 43.5 mmol). The mixture was heated for 15 min at 130 °C followed by 18 h at 150 °C, generating a light yellow solution. The mixture was cooled and treated with water (170 cm^3) to give a yellow suspension, which was washed with ether (3 × 80 cm^3). The aqueous solution was acidified with acetic acid, yielding a very light yellow precipitate upon cooling, which was filtered, washed with water, and dried thoroughly to yield the title compound as a pale yellow, crystalline solid. Yield: 5.90 g (83%). Mp: 170−2 °C. Anal. Calcd for $C_{13}H_{11}NO_2S$: C, 63.67; H, 4.49; N, 5.73; S, 13.06. Found: C, 63.68; H, 4.44; N, 5.60; S, 12.98. ^{1}H NMR (400 MHz, $CDCl_3$): δ 13.40 (1H, br s, −OH), 8.13 (1H, d, J = 8 Hz, H^4), 7.42−7.52 (5H, m, H$^{2'-6'}$), 7.09 (1H, d, J = 8 Hz, H^5), 2.23 (3H, s, CH_3); ^{13}C NMR (100 MHz, $CDCl_3$): δ 24.8 (CH_3), 119.8 (C^5), 121.4 (C^4), 129.6 (C^3), 130.1 (C$^{3',5'}$), 131.8 (C$^{1'}$), 136.1 (C$^{2',6'}$), 139.9 (C$^{4'}$), 160.4 (C^2), 160.8 (C^6), 167.4 (COOH). ESMS$^+$: m/z 246 (MH), 268 (MNa).

2-Methyl-1-azathioxanthone, 2. Polyphosphoric acid (60 cm^3) was added to 6-methyl-2-thiophenoxynicotinic acid (5.50 g 22.4 mmol) and the mixture heated at 120 °C for 4 h under argon with stirring. The resulting brown liquid was cooled to room temperature and then slowly poured onto cold concentrated aqueous sodium hydroxide solution (300 cm^3) with vigorous stirring. The light yellow precipitate that formed was collected via filtration. The product was recrystallized from warm EtOH. The crystals that formed upon standing were filtered and dried thoroughly to yield the title compound as a pale yellow crystalline solid. Yield: 4.61 g (90%). Mp: 145−7 °C. Anal. Calcd for $C_{13}H_9NOS$: C, 68.72; H, 3.89; N, 6.10; S, 14.00. Found: C, 68.43; H, 3.95; N, 6.17; S, 13.99. ^{1}H NMR ($CDCl_3$, 500 MHz): δ 8.73 (1H, d, J = 8.2 Hz, H^4), 8.60 (1H, d, J = 8 Hz, H^6), 7.65 (2H, m, H^{8,9}), 7.48 (1H, m, H^7), 7.31 (1H, d, J = 8.2 Hz, H^3), 2.70 (3H, s, CH_3). ^{13}C NMR (100 MHz, $CDCl_3$): δ 25.2 (CH_3), 121.7 (C^3), 124.8 (C^7), 127.3 (C^9), 127.5 (C^6), 129.6 (C$^{9'}$), 130.4 (C^4), 133.5 (C^8), 137.5 (C$^{6'}$), 138.5 (C$^{4'}$), 158.0 (C$^{1'}$), 162.1 (C^2), 181.0 (C^5). ESMS$^+$: m/z 228 (MH), 250 (MNa), 477 [2MNa].

2-Bromomethyl-1-azathioxanthone, 3. 2-Methyl-1-azathioxanthone (1.00 g, 4.41 mmol) was dissolved in CCl_4 (30 mL), and the reaction was heated to 80 °C under argon. *N*-Bromosuccinimide (392 mg, 0.5 equiv) was added along with benzoyl peroxide (10 mg) with stirring and the reaction monitored using TLC (SiO_2, toluene/DCM/MeOH, 49:49:2) and ^{1}H NMR, adding further NBS and benzoyl peroxide. After 15 h and the addition of 2.5 equiv of NBS, the crude reaction mixture was allowed to cool to room temperature and filtered. The solvent was removed under reduced pressure and the residue purified by column chromatography on silica gel (toluene/DCM, 90:10), to yield the product as a bright yellow crystalline solid. Yield: 0.57 g (42%). Mp: 190−2 °C. Anal. Calcd for $C_{13}H_8NOSBr$: C, 50.99; H, 2.62; N, 4.58; S, 10.46. Found: C, 51.13; H, 2.92; N, 4.81; S, 9.98. ^{1}H NMR (500 MHz, $CDCl_3$): δ 8.84 (1H, d, J = 8.1 Hz, H^4), 8.58 (1H, dd, J = 8.0 Hz, H^6), 7.65 (2H, m, H^{8,9}), 7.57 (1H, d, J = 8.1 Hz, H^3), 7.52 (1H, m, H^7), 4.61 (2H, s, CH_2Br). ^{13}C NMR (100 MHz, $CDCl_3$): δ 32.6 (CH_2), 121.8 (C^3), 125.8 (C^4), 126.7 (C^9), 127.2 (C^7), 129.1 (C$^{9'}$), 130.2 (C^6), 133.3 (C^8), 137.5 (C$^{6'}$), 139.2 (C$^{4'}$), 158.6 (C$^{1'}$), 161.1 (C^2), 180.6 (C^5). ESMS$^+$: m/z 306 (MH), 328 (MNa).

***trans*-Bis(Phe ester) Cyclen 4.** Under argon, 1,7-bis(benzyloxycarbonyl)-1,4,7,10-tetraazacyclododecane[19] (2.4 g, 4.5 mmol), *N*-(2-bromoacetyl)phenylalanine ethyl ester (3.2 g, 10.0 mmol), and potassium carbonate (8.5 g) in DMF (50 mL) were stirred at room temperature overnight. Then DCM (200 mL) was added, and the solution was washed with water (100 mL × 10) and dried over anhydrous potassium carbonate. The solvents were removed under reduced pressure, resulting in the *trans*-diCbz diamide compound as an oily product that was used directly in the next step without further purification. Yield: 4.3 g (98%). ^{1}H NMR ($CDCl_3$): δ 7.19−7.34 (20H, m, ArH); 5.08 (4H, s, $ArCH_2O$); 4.81 (2H, m, α-H (Phe)); 4.18 (4H, t, J = 7.2 Hz, OCH_2CH_3); 3.32 (8H, br s, cyclen); 3.11 (8H, br s, NCH_2 and $ArCH_2C$); 2.76 (8H, br s, cyclen); 1.19 (6H, t, J = 7.2 Hz, OCH_2CH_3). ^{13}C NMR (100 MHz, $CDCl_3$): δ 171.7, 170.8, 156.7, 136.6, 129.35, 129.25, 128.6, 128.55128.4, 128.2, 128.15, 126.8, 67.3, 61.3, 54.6, 53.1, 37.9, 14.1. HRMS: m/z calcd for $C_{50}H_{63}N_6O_{10}$(MH) 907.4536, found 907.4531.

The diester (4.1 g, 4.5 mmol) was dissolved in ethanol (50 mL) and hydrogenated over 0.1 g of Pd/C (20%, w/w) and 40 psi of hydrogen at room temperature for 4 days. The solvents were removed under reduced pressure, giving a colorless oil. The residue was recrystallized from ethyl ether and DCM, yielding a light yellow solid. Yield: 2.7 g (93%). ^{1}H NMR (400 MHz, $CDCl_3$): δ 7.30−7.15 (10H, m, ArH); 4.89 (2H, m, α-H (Phe)); 4.20 (4H, q, J = 7.2 Hz, OCH_2CH_3); 3.25 (8H, br s, NCH_2 CO, and $ArCH_2C$); 2.75 (16H, br s, cyclen); 1.30 (6H, t, J = 7.2 Hz, OCH_2CH_3). ^{13}C NMR (100 MHz, $CDCl_3$): δ 172.0, 170.4; 136.5, 129.5, 129.3, 128.4, 127.0; 61.7, 60.9; 53.1, 52.9; 47.4, 37.3, 14.1. HRMS: m/z calcd for $C_{34}H_{51}N_6O_6$(MH) 639.3800, found 639.3797.

L. Under argon, the diamide **4** (1.5 g, 2.2 mmol), 2-bromomethyl-1-azaxanthone (0.34 g, 1.1 mmol), and potassium carbonate (5 g) were stirred in acetonitrile (40 mL) at room temperature for 48 h. DCM

(19) Kovacs, Z.; Sherry, A. D. *J. Chem. Soc., Chem. Commun*. **1995**, 185.

(200 mL) was added, and the solution was washed with water (80 mL × 3) and dried over sodium sulfate. The product was purified by column chromatography on alumina with DCM/EtOAc/CH_3OH (250:15:4) as eluant, yielding a light yellow solid product. Mp: 66−8 °C. Yield: 0.32 g (34%). ^{1}H NMR (400 MHz, $CDCl_3$): δ 8.77 (1H, d, J = 8.0 Hz, H_1), 8.60 (1H, d, J = 8.0 Hz, H_8), 7.71−7.65 (2H, m, $H_5 + H_7$), 7.59−7.51 (2H, m, $H_2 + H_6$), 7.31−7.12 (10H, m, ArH); 4.81 (2H, dd, α-H (Phe)); 4.15 (4H, q, J = 7.2 Hz, OCH_2CH_3); 3.82 (2H, s, $ArCH_2N$); 3.26−3.16 (8H, m, cyclen); 3.04 (4H, s, NCH_2CO); 2.82 (4H, br s, cyclen); 2.77 (4H, br s, cyclen); 2.05 (4H, s, $ArCH_2C$); 1.23 (6H, t, J = 7.2 Hz, OCH_2CH_3). HRMS (ESMS$^+$): m/z calcd for $C_{47}H_{58}O_7N_7S$ (M^+) 864.4197, found 864.4191.

[EuL]$^{3+}$. The ligand (80 mg, 0.09 mmol) and $Eu(CF_3SO_3)_3$ (134 mg, 0.26 mmol) were boiled under reflux in acetonitrile (3 mL) for 36 h. The solution was added slowly to diethyl ether (500 mL) and filtered and the crude solid dissolved in a mixture of DCM (20 mL) and toluene (6 mL). The solution was allowed to slowly evaporate at room temperature; when most of the DCM had evaporated, a precipitate was collected, which was dried under vacuum, yielding a gray solid. Yield: 60 mg (44%). HRMS (ESMS$^+$): m/z calcd for $C_{49}H_{57}O_{13}N_7EuF_6S_3$ 1314.2305, found 1314.2311. UV/vis (H_2O): λ_{max} = 384 nm; λ_{em} = 446 nm (ligand fluorescence (ϕ_{em} = 44%), plus bands associated with Eu emission (ϕ_{em} = 9%). $\tau_{Eu}(H_2O)$ = 0.32 ms, $\tau_{Eu}(D_2O)$ = 0.49 ms, q = 1.1.

The Gd analogue was made by an analogous method. HRMS (ESMS$^+$): m/z calcd for $C_{49}H_{57}O_{13}N_7GdF_6S_3$ 1319.2321, found 1319.2379. r_{1p}(H_2O, 310 K, 60 MHz) = 7.3 mM^{-1} s^{-1}.

Cell Culture and Complex Loading. NIH 3T3, HeLa, or HDF cells were incubated under 5% carbon dioxide/air at 37 °C, in DMEM with 4.5 g/L glucose, L-glutamine, and pyruvate, supplemented with 10% natal bovine serum and a 1% penicillin/streptomycin mixture. For microscopy, cells seeded on coverslips were incubated with the complex dissolved in fresh medium at 37 or 4 °C in a 12-well plate for the indicated time. The cells were washed with PBS at least five times and mounted onto slides for measurements. For luminescence spectral measurement, the cells were incubated in a 100 mm Petri dish with the complex, washed with PBS at least five times, and then harvested with 1 mL of trypsin (0.25%, w/v). The mixture was diluted to 10 mL with PBS and centrifuged. The precipitates were collected and resuspended to 1.5 mL of PBS for spectral measurements. The cells were fixed by precooled methanol (−20 °C) for 15 min, washed with PBS for 5 min twice, and then loaded with the complex in DMEM as described above. For colocalization experiments, the complex (100 μM) was incubated with NIH 3T3 cells seeded on coverslips in DMEM for 4 h, and then the medium was replaced with fresh medium in the presence of SYTO dye (500 nM) for 30 min. The coverslips were then washed with PBS at least eight times and mounted onto slides for microscopy. The "fixed cells" were fixed by methanol prior to the above complex-loading procedure.

Cell viability studies were carried out by loading either the NIH 3T3 or HDF cells with complex (500 μM, 4 h) or with calcein-AM (5 μM, 30 min) and separately with both complex and dye. The cells were handled in a 12-well plate, washed with PBS, and mounted onto slides for examination as described above. Cells were examined by microscopy using the appropriate excitation and emission filters, so that the red europium emission and green calcein fluorescence could be distinguished separately. For the coloaded cells, emission was observed for >97% of the cells examined, corresponding to both the complex and the dye, and was judged to be indicative of good cell viability.

Acknowledgment. We thank EPSRC, the Royal Society, ONE-NE (Durham County Partnership/STBE), and the EC-EMIL and DiMI networks of excellence for support.

Supporting Information Available: Time course and concentration dependence of complex loading with NIH 3T3 cells, selected images of HeLa and HDF cells costained with RNA-Select and the europium complex, and absorption, luminescence, and CPL spectra of the complex in the presence of various anionic species. This material is available free of charge via the Internet at http://pubs.acs.org.

JA056303G